Mechanics & Industry

Numerical assessment of 3D macrodispersion in heterogeneous porous media

A. Beaudoin[1,a] and J.R. De Dreuzy[2,3]

[1] Institute P', University of Poitiers, France
[2] Institute of Environmental Analysis and Water Studies, Barcelona, Spain
[3] Géosciences, University of Rennes, France

Abstract – Hydrodynamic dispersion is a key controlling factor of solute transport in heterogeneous porous media. It critically depends on dimensionality. The asymptotic macrodispersion, transverse to the mean velocity direction, vanishes only in 2D and not in 3D. Using the classical Gaussian correlated permeability fields with a lognormal distribution of variance σ_Y^2, the longitudinal and transverse dispersivities are determined numerically as a function of heterogeneity and dimensionality. We show that the transverse macrodispersion steeply increases with σ_Y^2 underlying the essential role of flow lines braiding, a mechanism specific to 3D systems. The transverse macrodispersion remains however at least two orders of magnitude smaller than the longitudinal macrodispersion, which increases even more steeply with σ_Y^2. At moderate to high levels of heterogeneity, the transverse macrodispersion also converges much faster to its asymptotic regime than do the longitudinal macrodispersion. Braiding cannot be thus taken as the sole mechanism responsible for the high longitudinal macrodispersions. It could be either supplemented or superseded by stronger velocity correlations in 3D than in 2D. This assumption is supported by the much larger longitudinal macrodispersions obtained in 3D than in 2D, up to a factor of 7 for $\sigma_Y^2 = 7.56$.

Key words: parallel computing / transport equation / pure advection / heterogeneous media / 3d macrodispersion

1 Introduction

Hydrodynamic dispersion is a major component of solute transport in geological media controlling the relative solute distribution [1] as well as the mixing-induced chemical reactivity [2]. It results from the variability and the correlations of the velocity field over evolving scales from the pore scale to the field scale [3]. Hydrodynamic dispersion appears to be a Fickian process where the diffusion coefficient is replaced by an equivalent dispersion coefficient, which increases with time as the solute plume samples the heterogeneity field. The relation of geological heterogeneity to dispersion processes has been extensively analyzed in correlated multi-Gaussian log-permeability fields taken as an idealized model both simple enough to lead to general conclusions and complex enough to disclose some of the complex relationships between heterogeneity and dispersion [4]. The logarithm of permeability $Y(x) = \ln(K(x))$ is modeled by a normal distribution of variance σ_Y^2 following a

simple correlation pattern. Here, we will be considering a simple isotropic Gaussian correlation function such as $\langle Y'(x)Y'(x')\rangle = \sigma y^2 \exp(-(|x-x'|/\lambda)^2)$ where $Y'(x) = Y(x) - \langle Y \rangle$, $\langle \rangle$ marks the spatial average and λ is the correlation length. Whenever heterogeneities are bounded and their correlation limited, dispersion reaches an asymptotic regime characterized by an asymptotic dispersion coefficient also called macro-dispersion. Perturbation expansions of the flow and advection-diffusion equations have shown that macrodispersion is strongly anisotropic [5]. In the direction longitudinal to the mean velocity, the macrodispersion D_{LA} is proportional to the correlation length times the lognormal permeability variance : $D_{LA} = \langle v \rangle \lambda \sigma y^2$ with $\langle v \rangle$ the mean velocity. In the transverse directions, the macrodispersion D_{TA} is zero in the absence of local diffusion, i.e. when the local Peclet number is infinite or equivalently when velocity heterogeneities are the sole source of dispersion. These analytical estimates are valid both in 2D and in 3D for small enough permeability heterogeneities ($\sigma_Y^2 < 1$). They have been confirmed in 2D by numerous numerical studies [6] and have even been found to be robust for values of σ_Y^2 as high as 1.6 [7] and

a Corresponding author:
anthony.beaudoin@univ-poitiers.fr

even higher for spherical inclusion systems [8]. At higher heterogeneity levels ($1 < \sigma_Y^2 \leqslant 9$), the absence of transverse dispersion in 2D has been confirmed both by homogenization theory and numerical simulations [9]. The basic argument is that, in 2D without local diffusion, the solute plume is constrained within a given flow tube of finite and stable transverse dimension that strictly limits the dispersion. On the contrary for the longitudinal macrodispersion, numerical simulations have shown that it can be up to three times larger than the analytical estimate and that it scales with the square of σ_Y^2 for $\sigma_Y^2 \geqslant 2$ [10]. The strong increase of the macrodispersion likely comes the higher-order velocity correlations as the dependence of the velocity correlation on the velocity magnitude [11]. In 3D, full transport simulations on the linearized flow equation show that the transverse macrodispersion D_{TA} is significantly non zero [12], which proves to be consistent with predictions based on Corrsin's conjecture [13], and coarse-graining arguments [14]. For spherical inclusion systems, the transverse macrodispersion is also non vanishing but it remains small. It becomes critically larger for elongated ellipsoids [8]. If it has been well established that the transverse macrodispersion is non zero, open questions remain on its magnitude as well as on the magnitude of the longitudinal macrodispersion and on their behavior for higher heterogeneity levels ($\sigma_Y^2 > 1$). We address these issues with 3D extensive simulations of the full flow and transport equations that go far beyond the previous attempts [15].

2 Model and methods

The permeability field is generated within a rectangular parallelepiped of dimensions L_{L}, L_{T1} and L_{T2} at the same resolution Δ in all directions using a spectral method through the fftw library [16]. The indices "L", "T1" and "T2" stand for the three orthogonal directions of the parallelepiped and symbolized the direction "L" longitudinal to the main flow direction (defined just after) and the two directions "T1" and "T2" orthogonal to it. The flow equation $\nabla (K \nabla h) = 0$ is solved with fixed heads h_+ and h on the faces orthogonal to the longitudinal direction L. Periodic boundary conditions on the other transverse faces minimize the perturbation of the flow field generally reported by no-flow boundary conditions [17]. The flow equation is discretized by a finite-volume scheme and the resulting linear system is solved with the parallel algebraic multigrid method of HYPRE [18]. Velocities $\boldsymbol{v}$ at the grid centers are derived from the hydraulic head h by Darcy's law $\mathbf{v} = -K/\theta \nabla h$. Porosity θ is chosen uniform and the mean flow velocity $\langle \boldsymbol{v} \rangle$ is parallel to the L direction. Its norm $\langle v \rangle$ is equal to (K_{eq}/θ) $|h_+ - h_-|/L_L$ with K_{eq} the equivalent permeability [19]. Transport is restricted to the sole advection process and is simulated by a first-order explicit particle tracking method [20]. Between t and $t + dt$, a particle moves from positions $\mathbf{x}(t)$ to $\mathbf{x}(t + dt)$ according to $\mathbf{x}(t + dt) = \mathbf{x}(t) + \mathbf{v}[\mathbf{x}(t)]\,dt$ where the velocity $\mathbf{v}$ in each

point is obtained with a linear interpolation in each direction on the grid [21]. The time step dt is adapted along the particle trajectory to the magnitude of the local velocity so that the particle takes on average 10 steps within each grid cell [22]. Particles are injected on a large plane of size $0.8\ L_{\mathrm{T1}} \times 0.8\ L_{\mathrm{T2}}$ orthogonal to the L direction located at least at five correlation lengths downstream from the side of the system to avoid border effects on the velocity statistics. Particles are injected proportionally to the flow through the plane to speed up the convergence to the asymptotic regime. Effective dispersivities derived from the dispersion coefficient divided by the mean velocity $\langle v \rangle$ normalized by λ (dispersion coefficients divided by the mean velocity $\langle v \rangle$ and λ) are determined from N_{R} realizations of the permeability field with N_{P} particles for each realization according to:

$$\alpha_k(t) = \frac{1}{2\lambda \langle v \rangle} \frac{1}{N_R}$$
$$\times \sum_{i=1}^{N_R} \frac{d}{dt} \left[\frac{1}{N_p} \sum_{j=1}^{N_p} x_k^{j,i}(t)^2 - \left(\frac{1}{N_p} \sum_{j=1}^{N_p} x_k^{j,i}(t) \right)^2 \right] \tag{1}$$

where $x_k^{j,i}$ is the position of the particle j in simulation i in direction k at time t. For consistency we have normalized the time t by $\lambda/\langle v \rangle$ and kept the same notation t for simplicity. As we have systematically checked that $\alpha_{\mathrm{T1}} = \alpha_{\mathrm{T2}}$, we report results only for one of them that we generically denote α_{T}. To reach large enough domain sizes and number of simulations, all numerical methods have been implemented in parallel [23]. More details on the methods and implementation can be found in previous studies on 2D macrodispersion [24].

3 Results and discussion

At low to moderate levels of heterogeneities ($\sigma_Y^2 \leqslant$ 2.25), the asymptotic values of macrodispersivities α_{LAM} and α_{TAM} are compared to those obtained fully analytically by perturbative analysis [5] and half analytically by full transport simulations on a first-order approximation of the velocity field [12, 25] (Figs. 1 and 2). The numerically obtained macrodispersivities are closer to those of Gelhar et al. [5] in the longitudinal direction and to those of Dentz et al. [25] and Schwarze et al. [12] in the transverse direction. At moderate to high levels of heterogeneities ($\sigma_Y^2 \geqslant 1$), the transverse macrodispersivity is significantly non zero as previously demonstrated [9] and strongly increases with σ_Y^2 (Fig. 2). More precisely it increases quadratically in σ_Y^2 for $\sigma_Y^2 \geqslant 1$ (dashed line compared to black squares):

$$\alpha_{\mathrm{TAM}} \approx \alpha_{\mathrm{TAM}}(1)\ \sigma_Y^4 \tag{2}$$

The longitudinal macrodispersivity is much larger both to the linear prediction of Gelhar and Axness [5] and to the 2D equivalent macrodispersivities (Fig. 1). The strong
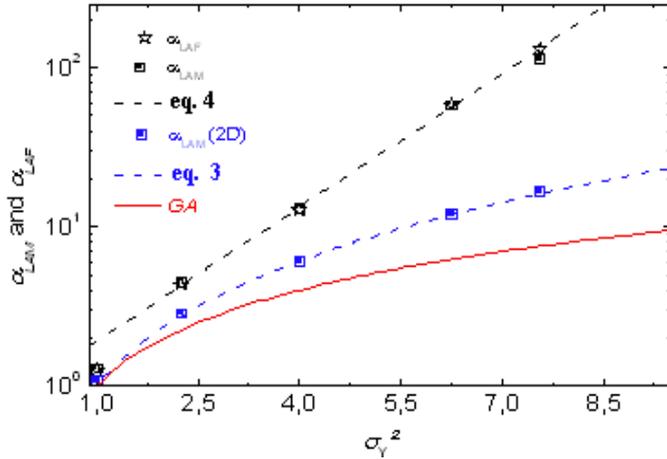
Fig. 1. Longitudinal macrodispersivity α_{LAM} as function of σ_Y^2 (the longitudinal macrodispersivity is compared to the values obtained numerically for equivalent 2D systems (blue squares) and to the perturbative approximation [5] (red line)).
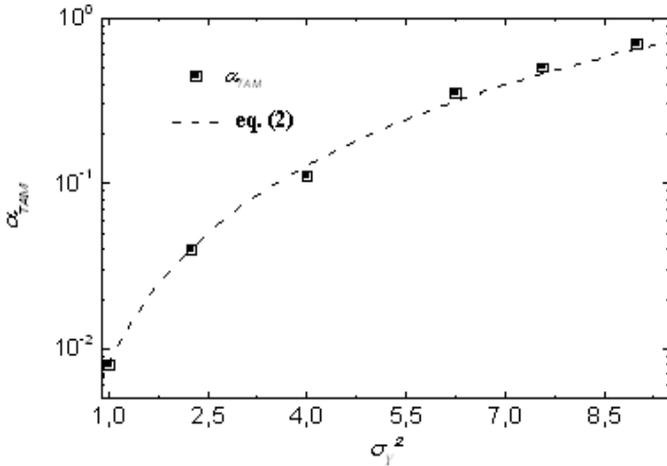
Fig. 2. Transverse macrodispersivity α_{TAM} as function of σ_Y^2.

difference to the full perturbative solution is expected as it was already the case in 2D. The large differences between the 2D and the 3D cases show that the Euclidean dimension does not only impact the transverse macrodispersivity but also the longitudinal one. The 3D longitudinal macrodispersivity is twice larger than the 2D one for $\sigma_Y^2 = 2.25$ and 7 times larger for $\sigma_Y^2 = 7.56$. More globally, the 2D and 3D longitudinal macrodispersivities display different dependencies with σ_Y^2. In 2D, the longitudinal macrodispersity increases first linearly and then quadratically with σ_Y^2 at high heterogeneities [10] (Fig. 1):

$$\alpha_{LAM}(2D) \approx 0.84\,\sigma_Y^2 + 0.17\,\sigma_Y^4 \qquad (3)$$

The coefficient in front of the linear and quadratic terms are only slightly different from those obtained with an exponentially correlated permeability field [10]. In 3D, as shown previously, α_{LAM} increases rather exponentially than quadratically with σ_Y^2 for $\sigma_Y^2 \geqslant 2.25$ (Fig. 1):

$$\alpha_{LAF} \approx \exp\left(\sigma_Y^2/1.55\right). \qquad (4)$$

While the longitudinal and transverse macrodispersivities display very different types of variations, their rate $\alpha_{LAM}/\alpha_{TAM}$ is less variable between 100 and 200, close to the value of 250 obtained for spherical inclusions at $\sigma_Y^2 = 4$ [8]. It remains very high showing that the longitudinal macrodispersivity is at least 2 orders of magnitude larger than the transverse macrodispersivity. We conclude that the longitudinal macrodispersivity increases exponentially with σ_Y^2 at high heterogeneity levels. The increase is much stronger than both the linear increase predicted by perturbative analysis and the quadratic increase characteristic of its 2D counterpart. The transverse macrodispersivity is significantly positive (non zero) and increases quadratically with σ_Y^2. The longitudinal macrodispersivity remains always two orders of magnitude larger than the transverse macrodispersivity.

References

[1] P.G. Saffman, A theory of dispersion in a porous medium, J. Fluid Mech. 6 (1959) 321−349

[2] J.-R. de Dreuzy, J. Carrera, M. Dentz, T. Le Borgne, Time evolution of mixing in heterogeneous porous media, Water Resour. Res. 48 (2012b) W06511

[3] G. Taylor, Dispersion of Soluble Matter in Solvent Flowing Slowly through a Tube, Proc. Roy. Soc. London Ser. Math. Phys. Sci. 219 (1953) 186−203

[4] R.A. Freeze, Stochastic-conceptual analysis of one-dimensional groundwater flow in nonuniform homogeneous media, Water Resour. Res. 11 (1975) 725−741

[5] L.W. Gelhar, C.L. Axness, Three-dimensional stochastic analysis of macrodispersion in aquifers, Water Resour. Res. 19 (1983) 161−180

[6] Y. Rubin, Stochastic modeling of macrodispersion in heterogeneous porous media, Water Resour. Res. 26 (1990) 133−141

[7] A. Bellin, P. Salandin, A. Rinaldo, Simulation of dispersion in heterogeneous porous formations: statistics, first-order theories, convergence of computations, Water Resour. Res. 28 (1992) 2211−2227

[8] I. Jankovic, A. Fiori, G. Dagan, Flow and transport in highly heterogeneous formations: 3. Numerical simulations and comparison with theoretical results, Water Resour. Res. 39 (2003) 1270

[9] I. Lunati, S. Attinger, W. Kinzelbach, Macrodispersivity for transport in arbitrary nonuniform flow fields: asymptotic and preasymptotic results, Water Resour. Res. 38 (2002) 1187

[10] J.-R. de Dreuzy, A. Beaudoin, J. Erhel, Asymptotic dispersion in 2D heterogeneous porous media determined by parallel numerical simulations. Water Resour. Res. 43 (2007) W10439

[11] T. Le Borgne, J.-R. de Dreuzy, P. Davy, O. Bour, Characterization of the velocity field organization in heterogeneous media by conditional correlations, Water Resour. Res. 43 (2007) W02419

[12] H. Schwarze, U. Jaekel, H. Vereecken, Estimation of Macrodispersion by Different Approximation Methods for Flow and Transport in Randomly Heterogeneous Media, Transport in Porous Media 43 (2001) 265−287

[13] S.P. Neuman, Y.-K. Zhang, A Quasi-Linear Theory of Non-Fickian and Fickian Subsurface dispersion 1. Theoretical Analysis With Application to Isotropic Media, Water Resour. Res. 26 (1990) 887−902

[14] S. Attinger, M. Dentz, W. Kinzelbach, Exact transverse macro dispersion coefficients for transport in heterogeneous porous media, Stoch. Environ. Res. Risk Assess. 18 (2004) 9−15

[15] A.F.B. Tompson, L.W. Gelhar, Numerical simulation of solute transport in three-dimensional, randomly heterogeneous porous media, Water Resour. Res. 26 (1990) 2541−2562

[16] A.L. Gutjahr, Fast Fourier transforms for random field generation: New Mexico Tech project report 4-R58-2690R, New Mexico Institute of Mining and Technology, 1989

[17] P. Salandin, V. Fiorotto, Solute transport in highly heterogeneous aquifers, Water Resour. Res. 34 (1998) 949−961

[18] J.-E. Roberts, J.-M. Thomas, Mixed and hybrid methods, in Handbook of Numerical Analysis 2, Finite Element Methods -part 1, P.G. Ciarlet, J.L. Lions (eds.), Elsevier Science Publishers B.V. North-Holland, 1991 pp. 523−639,

[19] Matheron, Eléments Pour une Théorie des milieux Poreux, Masson, Paris, 1967

[20] N.G. Van Kampen, Stochastic Processes in Physics and Chemistry, Elsevier Science Pub Co., 1981

[21] D.W. Pollock, Semianalytical computation of path lines for finite-difference models, Ground Water 26 (1988) 743−750

[22] X.H. Wen, J.J. Gomez-Hernandez, The constant displacement scheme for tracking particles in heterogeneous aquifers, Ground Water 34 (1996) 135−142

[23] A. Beaudoin, J.R. de Dreuzy, J. Erhel, H. Mustapha, Parallel Simulations of Underground Flow in Porous and Fractured Media, Proceedings of the International Conference ParCo, John von Neumann Institute for Computing, Jülich, 2005

[24] A. Beaudoin, J.-R. de Dreuzy, J. Erhel, A comparison between a direct and a multigrid sparse linear solvers for highly heterogeneous flux computations, paper presented at European Conference on Computational Fluid Dynamics, ECCOMAS CFD, 2006

[25] M. Dentz, H. Kinzelbach, S. Attinger, W. Kinzelbach, Temporal behavior of a solute cloud in a heterogeneous porous medium: 3. Numerical simulations, Water Resour. Res. 38 (2002) 1118